Article

Phytochemical Substances – Mediated Synthesis of Zinc Oxide Nanoparticles (ZnO NPS)

Fawzeeh Nayif Alharbi , Zulfa Mohamed Abaker * , Suzan Zein Alabdeen Makawi

Posted Date: 5 July 2023

doi: 10.20944/preprints202307.0314.v1

Keywords: Artemisia absinthium; green ZnO NPs; band gap energy; plant extract; phytochemicals

Article

Phytochemical Substances —Mediated Synthesis of Zinc Oxide Nanoparticles (ZnO NPS)

Fawzeeh Nayif Alharbi [1], Zulfa Mohamed Abaker [2,3,*] and Suzan Zein Alabdeen Makawi [2,4]

[1] Department of Chemistry, College of Science, Qassim University, Buraidah 51452, Saudi Arabia; Wfwfw77@gmail.com
[2] Department of Chemistry, College of Science and Arts, Qassium University, Ar Rass 51921, Saudi Arabia; suzanmakawi@yahoo.com
[3] Department of Chemistry & Industrial Chemistry, College of Applied and Industrial Sciences, Bahri University, Khartoum P.O. Box 12327 11111, Sudan
[4] Department of Chemistry, Faculty of Science and Technology, Alneelain University, Khartoum11121, Sudan
* Correspondence: zulfa.abaker@gmail.com

Abstract: *Artemisia absinthium* (*A. absinthium*) leaf extract was successfully used to create zinc oxide nanoparticles (ZnO NPs), and their properties were investigated via several techniques, including X-ray diffraction (XRD), scanning electron microscopy (SEM), energy-dispersive X-ray (EDX), Fourier transform infrared (FTIR), and UV–Vis spectroscopy. SEM analysis confirmed the spherical and elliptical shapes of the particles. Three different zinc peaks were observed via EDX at energies of 1, 8.7, and 9.8 keV, together with a single oxygen peak at 0.5 keV. XRD analysis identified ZnO NPs as having a hexagonal wurtzite structure with a particle size that decreased from 24.39 to 18.77 nm, and with an increasing surface area (BET) from 4.003 to 6.032 m^2/g for the ZnO (without extract) and green ZnO NPs, respectively. FTIR analysis confirmed the groups of molecules that were accountable for stabilizing and minimizing the ZnO NPs, which was apparent at 3400 cm. Using UV–Vis spectroscopy, the band gap energies (Egs) for the green ZnO and ZnO (without extract) NPs were estimated, and the values were 2.65 and 2.79 eV, respectively.

Keywords: *Artemisia absinthium*; green ZnO NPs; band gap energy; plant extract; phytochemicals

1. Introduction

The most recent fields to develop and expand rapidly are nanoscience and nanotechnology. Nanomaterials are used in a variety of industries, including in the electrical and electronics, textile, cosmetic, and medicinal sectors. Nanomaterials are materials that are generated using nanotechnologies; these include NPs with sizes between 1 and 100 nm. In industrial settings, metal NPs and metal oxides are commonly needed. Some of the different kinds of metal and metal oxide NPs with multiple uses are aluminum, nickel, silver, copper, copper oxide, iron, iron oxide, cerium dioxide, titanium dioxide, and zinc oxide [1–3]. NPs are produced using a number of physical, chemical, and biological methods; however, these chemical and physical processes frequently need a lot of energy, and can produce dangerous and poisonous substances, that can result in additional risks [4]. In order to deal with these issues, current researchers have created biotechnology or "green" technology, which uses plant substances with low levels of the chemicals as a reliable, inexpensive, and safe synthesis method.

ZnO NPs have attracted more interest compared to the other metal oxides due to their safe and low-cost manufacturing and preparation methods [5,6]. ZnO has numerous uses in the domains of engineering, biology, and medicine. Many engineering applications exist for ZnO NPs, including solar cells [7], photodetectors, biosensors [8], chemical sensors [9], and gas sensors. Furthermore, ZnO NPs exhibit cytotoxic, antibacterial, and fungicidal properties in biological and medical applications [10,11]. They also have chemiluminescent properties [12], and wound-healing, antidiabetic and anti-inflammatory activities [10,13]. ZnO, a material that is capable of displaying a variety of

 doi:10.20944/preprints202307.0314.v1

nanostructures, has exceptional semiconducting, visual, and dielectric capabilities. As a result, research has conducted on ZnO-based nanomaterials for a variety of uses, including electronic and optical devices, energy storage, cosmetics, nanosensors, etc. [14]. ZnO has a broad band gap semiconductance (3.37 eV) and a high excited-state binding energy (60 meV), which lead to its extremely efficient excitonic blue and near-UV emission [14,15]. ZnO has been given FDA approval for use in sunscreens due to its stability and innate ability to absorb ultraviolet (UV) radiation [17,18].

The method of choice for nanoparticle synthesis is plant-based, which is simple to generate and establish [18]. The synthesis of NPs, particularly using phytochemicals, is a recent development that is considered straightforward, affordable, and harmless [19]. Conventional methods for the production of nanoparticles have disadvantages, namely their lengthy processing times, costs, and their usage of hazardous substances. Due to these restrictions, the majority of relevant studies concentrated on green and quick synthesis techniques for the creation of nanoparticles [21,22]. Plant-based techniques have been acquired as environmentally friendly since these techniques create items and byproducts that are eco-friendly. Additionally, they use less energy, do not utilize expensive chemicals, and produce more; green methods are promoted as being economical [22]. Due to the availability of phytochemicals and numerous bioactive compounds with numerous functional groups, including polyphenols, flavonoids, terpenoids, carboxylic acids, quinones, aldehydes, ketones, and amides, phytochemicals are capable of being utilized to create nanoscale reduction agents [23,24]. These phytochemicals reduce metal ions into nano form through a reduction mechanism [25]. Many types of plants have been used in the manufacturing of ZnO NPs, namely, aloe vera [26], moringa oleifera leaf extract [27], Ocimum basilicum [28], rosemary leaves [29], azadirachta indica leaves [30], Lycopersicon esculentum (tomato) [31,32], etc.

A. absinthium is among the therapeutic plants that are used in traditional health care, and numerous studies have been conducted on it to determine the extent to which it has inhibitory and antibacterial properties. A thorough review of the literature on *A. absinthium's* phytochemical data reveals that their principal constituents are polyphenolics, terpenoids, flavonoids, coumarins, caffeoylquinic acids, sterols, and acetylenes, which are responsible for the reduction process [33–35].

The main objective of this investigation was to produce ZnO nanostructures utilizing the fresh leaves of *A. absinthium* extract as a dispersion and reduction agent. Additionally, *A. absinthium* extract and ultrasonic energy were combined to check for any product alterations. The nanoparticle's presence was then verified using XRD, SEM, EDX, FTIR, and UV. Vis.

2. Materials and Methods

2.1. Materials

A. absinthium leaves were collected from a home garden in Al-Qassim Al-Rass, Saudi Arabia. Zinc nitrate (Zn $(NO_3)_2.6H_2O$) was obtained from LOBA Chemie, and KOH was obtained from Techno Pharmchem, India.

2.2. Methods

2.2.1. Plant Extract

The method was adapted from Rasli et al. [26] and M. Ali et al. [36], with some modifications. Approximately 50 g of fresh *A. absinthium* leaves was cleaned with distilled water before being chopped into pieces and crushed with 500 mL of distilled water into a slurry using a pastille. The mixture was heated at 70 °C for ½ h using a magnetic stirrer. The extract was allowed to cool to ambient temperature before being filtered through Whatman No. 1 filter paper and kept in a refrigerator at 4 °C for use in subsequent experiments (reducing and capping agents).

2.2.2. Green Synthesis of ZnO NPs

As show in Figure 1. ZnO NPs were created using a direct precipitation technique. Aqueous solutions were prepared using Zn $(NO_3)_2.6H_2O$ (10 g in 100 mL of deionized water) and 0.5 M KOH

Preprints (www.preprints.org) | NOT PEER-REVIEWED | Posted: 5 July 2023 doi:10.20944/preprints202307.0314.v1

(2.8 g in 100 mL of deionized water). A small amount of KOH was gradually added to 90 mL of Zn $(NO_3)_2.6H_2O$ to bring the mixture up pH 12. A volume of 10 mL of plant aqueous extract was added while being vigorously stirred and kept at a temperature of 90 °C using a magnetic stirrer for 2 h until the suspension was created. After that, it was sonicated at 500 Hz for 20 min, resulting in a yellow precipitate. The precipitate was repeatedly rinsed with water and ethanol before being dried in a hot-air oven for an entire night at 90 °C. The precipitate was calcined for 2 h at 500 °C in a muffle furnace. The same method was repeated with Zn $(NO_3)_2.6H_2O$ without adding plant extract**.** The method is adapted from M. Ali et al., with a few modifications [36].

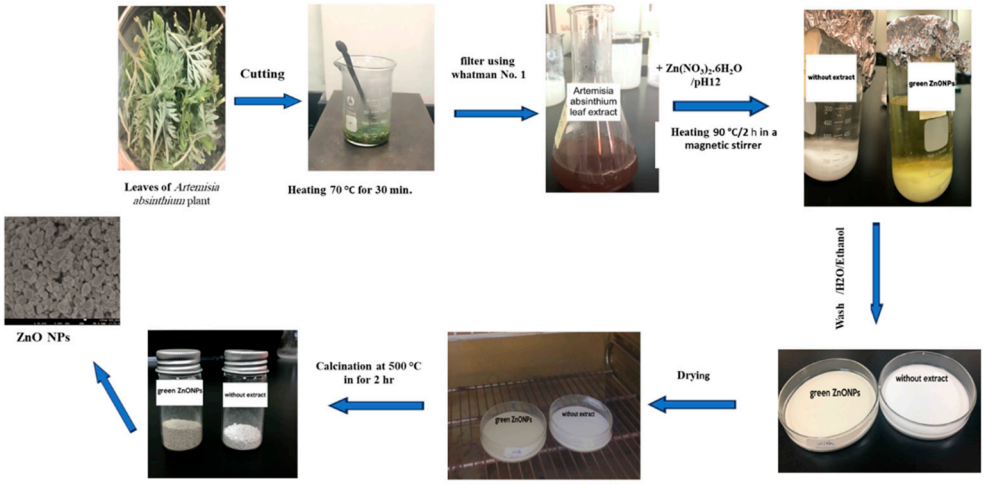

Figure 1. Green synthesis of ZnO NPs

2.3. Characterization Techniques

2.3.1. Characterization of Artemisia absinthium Extract

Two techniques were used to detect the active components in the plant extract: reagent-based qualitative analysis, followed by drying and analysis with FTIR (SHIMADZU).

Flavonoids Test

A volume of 1 mL of NaOH was added to 1 mL of plant extract; the development of a bright yellow color provides evidence of the existence of flavonoids.

Wagner's Test

A volume of 1 mL of 1.5% *v*/*v* HCl was used to acidify the plant extract before Wagner's reagent was added. The production of a brown color served as a sign that alkaloids were present.

Frothing Test

A volume of 1 mL of the plant extract was diluted individually with 5 mL of distilled water and shaken for 15 min. The formation of a thick layer of foam shows evidence of saponins.

Ferric Chloride Test

Neutral ferric chloride ($FeCl_3$), 5%, was added to 1 mL of the plant extract. The presence of tannins and phenolic compounds is indicated by the production of a dark blue or bluish-black colored product.

2.3.2. Characterization of ZnO NPs

In order to investigate the ZnO NPs, several analytical methods were adopted.

Preprints (www.preprints.org) | NOT PEER-REVIEWED | Posted: 5 July 2023 doi:10.20944/preprints202307.0314.v1

XRD—Diffraction Analysis

An X-ray diffractometer (XRD, Rigaku with K beta filter, time duration 10.000°/min, scanning range 10.0–90.0° and operated at 40 kV, 40 mA) was used to examine the crystal size. The well-known Scherer formula was used to calculate the typical crystal size, D.

$$D = \frac{K\lambda}{\beta \cos \theta} \ldots\ldots\ldots\ldots\ldots\ldots\ldots\ldots\ldots\ldots\ldots\ldots\ldots\ldots\ldots\ldots\ldots\ldots\ldots.. \text{Scherer equation}$$

Here, λ is the wavelength (0.154 nm); β is the full width at half-maximum (FWHM) in radians and K is a constant equal to 0.90; θ is the diffraction angle.

SEM and EDX Analysis

EDX analysis was used to determine the elementary calculation, while SEM (FESEM, JEOL-SEM, 6700F) was used to examine the surface morphology of the NPs.

FTIR Analysis

A Perkins Elmer FTIR spectrometer (4000–400 cm^{-1}) was used to identify the functional groups using the KBr technique.

UV–Vis Analysis

A UV-2550 (Shimadzu, Tokyo, Japan) with a scanning range from 200 to 800 nm was used to monitor the diffuse reflection/absorption spectra (DRS), and to calculate the bandgap energy.

3. Results and Discussion

3.1. Characterization of A. absinthium Leaf Extract

3.1.1. Identification of Active Ingredients

The generated plant extract works as a stabilizing as well as a decreasing agent; it contains a large amount of polyphenols, which, in turn, consist of flavonoids, antibiotics, antioxidants, and organic aggregates. When this extract added to zinc salt, it breaks the (OH) bond and forms a partial bond with the metal; when this partial bond is broken, the electrons move to form zinc hydroxide, which in turn reacts with (OH) coming from sodium hydroxide to form nanoscale zinc oxide. Due to the availability of the OH groups for the production of NPs, flavonoids and tannins are the primary phytochemical component of *Artemisia absinthium* extract, which are visible bioactive minimizing and stabilizing agents [37]. The *Artemisia absinthium* extract was subjected to phytochemical analysis using a variety of reagents to identify several types of bioactive substances. The most significant active components found are outlined in Table 1. Figure 2. explain the role of the plant extract in reducing metal salt into nanoparticle.

Table 1. Phytochemical analysis of plant extract.

No.	Active Components	Test	Result
1	Phenolics	$FeCl_3$	+
2	Alkaloids	Wagner's reagent	+
3	Saponins	foam test	+
4	Flavonoids	alkaline test	+

Preprints (www.preprints.org) | NOT PEER-REVIEWED | Posted: 5 July 2023 doi:10.20944/preprints202307.0314.v1

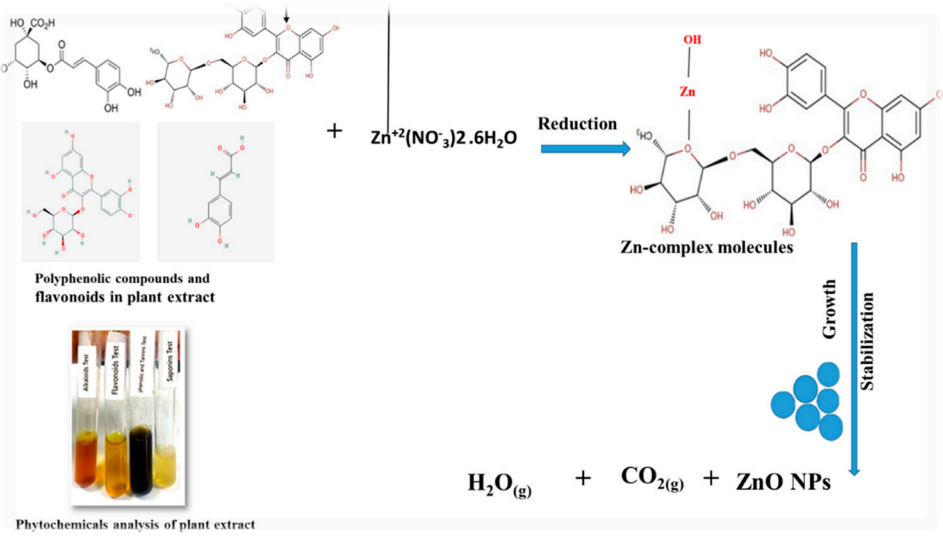

Figure 2. Reduction of the active components to zinc salts.

3.1.2. FTIR Analysis

The spectrum of the plant extract was determined after it was dried from water at room temperature. Figure 3 represents the infrared peaks of the plant extract. The results show that the absorption bands at 3400, 1608, and 1063 cm^{-1} belong to the stretching vibrations of OH, C=O, and C-O, respectively, which confirmed the presence of polyphenolic substances that can serve as minimizing and stabilizing agents.

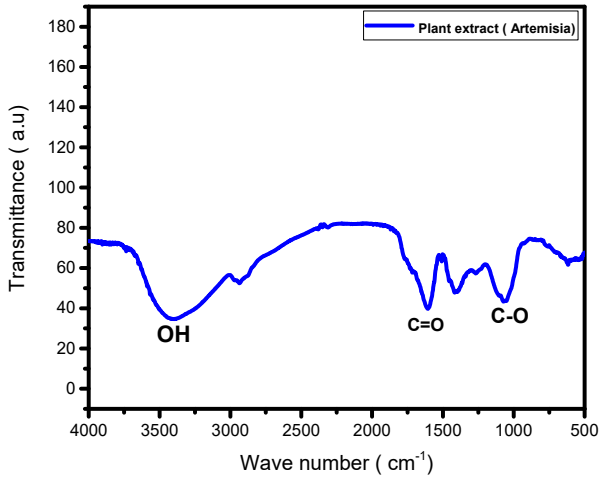

Figure 3. FTIR analysis of plant extract.

3.2. Characterization of ZnO NPs

3.2.1. X-ray Diffraction

The materials' particle size and crystallinity were evaluated using XRD analysis. The structural properties of the prepared NPs are shown in Figure 4. Compared with the data from JCPDS Card No. 36-1451, there was no sign observed of a peak impurity or secondary phase. The strong and narrow diffraction peaks, especially (100) (002) and (101), showed good crystal structure and high-quality intensities of the peaks. Sharp extreme peaks about 2θ at the numbers 31.84, 34.49, 36.32, 47.62, 56.68, 62.95, 66.48, 68.04, 69.17, corresponded to the planes of (100), (002), (101), (102), (110), (103), (200), (112) and (201) orientations, respectively, for ZnO NPs (without extract); meanwhile, the 2θ values

Preprints (www.preprints.org) | NOT PEER-REVIEWED | Posted: 5 July 2023 doi:10.20944/preprints202307.0314.v1

for green ZnO appeared at 31.82°, 34.47°, 36.30°, 47.60°, 56.67°, 62.93°, 68.03°, 69.154°, corresponding to the planes of (100), (002), (101), (102), (110), (103), (200), (112) and(201)orientations, respectively.

The strong peak in direction (101) indicated that the nanomaterial prepared was in the hexagonal wurtzite phase. These findings demonstrated similar types of peak indices for the crystalline nature of ZnO NPs produced in study carried out by [38].

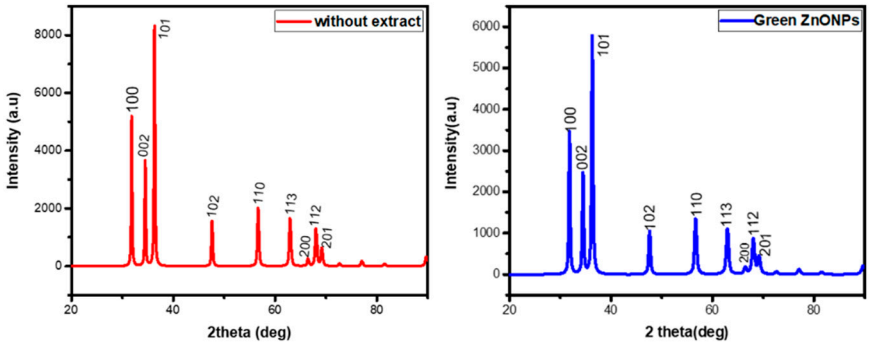

Figure 4. XRD spectra of without extract and green ZnO NPs.

The average crystallite sizes of the ZnO NPs (without extract) were calculated from the XRD data of Figure 4 using the Scherrer formula.

$$D = \frac{0.90\lambda}{\beta cos\theta} \quad \text{.....(Scherrer formula)}$$

The calculated crystallite size values listed in Table 2.

Table 2. Particle sizes of ZnO NPs (without extract) from Figure 4.

No. of Peaks	Indices	Location (2θ)	FWHM (2θ)	Size (nm)
1	100	31.8405	0.25611	32.25
2	002	34.4993	0.27379	30.38
3	101	36.3291	0.28256	29.59
4	102	47.6240	0.34103	25.46
5	110	56.6831	0.3981	22.67
6	113	62.9548	0.43834	21.25
7	200	66.4807	0.48187	19.71
8	112	68.0481	0.48285	19.85
9	201	69.1720	0.52439	18.40
			Average size	24.39

The average crystallite sizes of the green ZnO NPs were calculated from the XRD data of Figure 4 using the Scherrer formula. The calculated values for crystallite size are listed in Table 3.

Table 3. Particle sizes of green ZnO NPs from Figure 4.

No. of Peaks	Indices	Location (2θ)	FWHM (2θ)	Size (nm)
1	100	31.8216	0.34989	23.61
2	002	34.47333	0.37528	22.16
3	101	36.30893	0.37771	22.13
4	102	47.60253	0.4578	18.96
5	110	56.67089	0.54533	16.55
6	113	62.93347	0.60605	15.36
7	200	66.56221	0.66134	14.37
8	112	68.03501	0.69904	13.71
9	201	69.15222	0.43528	22.16

Preprints (www.preprints.org) | NOT PEER-REVIEWED | Posted: 5 July 2023 doi:10.20944/preprints202307.0314.v1

	Average size	18.77

The calculated average crystallite size values of ZnO NPs (without extract) and green ZnO NPs were 24.39 and 18.77, respectively. It was observed that the average crystallite size was reduced in the green ZnO NPs. This demonstrates how the plant extract works to convert nickel nitrate salt to nickel oxide, and the study's findings are consistent with those of earlier research [7,40].

3.2.2. FTIR Analysis

Figure 5 shows the resulting nanoparticles' spectra analyzed with FTIR. The spectrum green ZnO NPs showed a significant decrease in the intensity of the peak at around 3400 cm^{-1} when compared with the spectrum of the plant extract (Figure 3); this indicates the vital role of biomolecules attributed to this functional group in minimizing ZnO. The new broad absorption bands observed at 439.77 and 432.05 cm^{-1} for the ZnO (without extract) and green ZnO NPs, respectively, supporting ZnO NP production. These findings are consistent with those of earlier research [40].

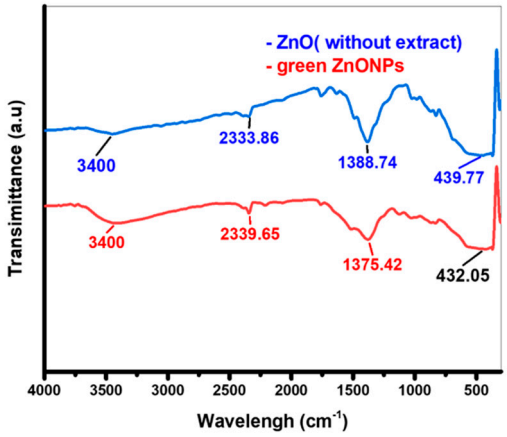

Figure 5. FTIR spectra of ZnO without extract and green ZnO NPs.

3.2.3. SEM Analysis

The spectra that resulted from examination of the surface morphology (shape) are shown in Figure 6. The observed outcomes made it abundantly evident that ZnO without extract and the green ZnO NPs showed different agglomerated particles. Low-magnification pictures captured in Figure 6a,c clearly show that the aggregated particles did not entirely separate, whereas those captured at higher magnification in Figure 6b,d show clear images ranging from spherical to rod-like and sheet-like structures. These findings were consistent with those of earlier research [41,42].

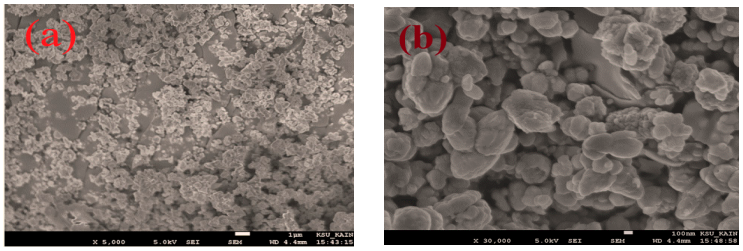

Preprints (www.preprints.org) | NOT PEER-REVIEWED | Posted: 5 July 2023 doi:10.20944/preprints202307.0314.v1

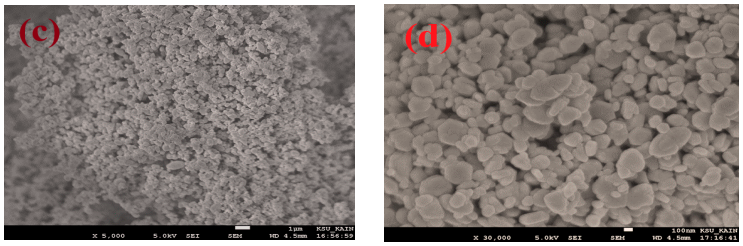

Figure 6. SEM images (**a**,**b**) for ZnO without extract (**c**,**d**) for green ZnO NPs.

3.2.4. EDAX Analysis

X-ray (EDX) techniques were used to further explore the samples, in order to gain additional insight into the topographies of the ZnO NPs. The spectra shown in Figure 7 show three distinct zinc peaks at energies of 1 keV, 8.7 keV, and 9.8 keV, respectively, as well as a single oxygen peak at 0.5 keV, all related to ZnO nanoparticles. The majority of the sample was ZnO, as seen by the zinc and oxygen peaks' high intensities [43].

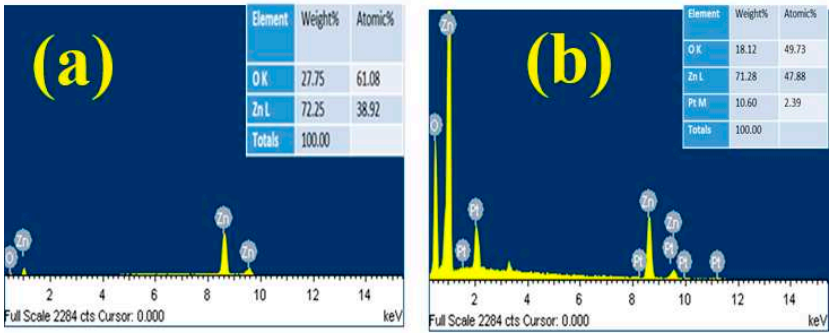

Figure 7. EDX spectra of (**a**) ZnO (without extract) and (**b**) green ZnO NPs.

3.2.5. DRS Analysis

The optical characteristics and band gap energy values of the produced NPs are displayed in Figure 8a,b. The absorption bands for ZnO (without extract) and green ZnO NPs were observed at 346 and 366 nm, respectively. These results are consistent with those reported in the literature [44].The band gap energy values of the samples were calculated by expanding the graph's linear component and plotting $(\alpha hv)^2$ versus energy (Eg), as shown in Figure 8b. The Tauc equation was used to determine the samples' band gap energy values [44].

$$\alpha(h\upsilon)^2 = A(h\upsilon - Eg) \quad \text{.....(Tauc equation)}$$

Here, α is the absorption coefficient, h is Planck's constant, ν is the frequency, Eg is the band gap energy and A is a proportionality constant. For the ZnO (without extract) and green ZnO NPs, the computed Eg values were 2.79 and 2.65, respectively [45].

Preprints (www.preprints.org) | NOT PEER-REVIEWED | Posted: 5 July 2023 doi:10.20944/preprints202307.0314.v1

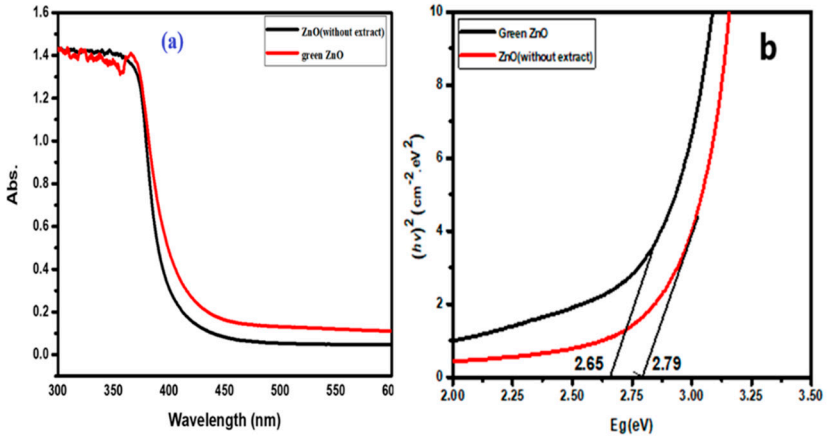

Figure 8. (**a**) UV–Vis spectra; (**b**) Tauc plots of ZnO (without extract) and green ZnO NPs.

3.2.6. BET Determination

Surface area (BET) was used to calculate the precise surface area of the prepared nanomaterial. Figure 9 shows nitrogen adsorption–desorption isotherms of the produced nanomaterial. The isotherm shows how the NPs behaved as a typical type (IV) isotherm with a deceleration loop in the low-pressure area ($P/P_0 < 0.8$), which is characteristic of mesoporous nanostructures. Table 4 shows the BET, pore volume, and average pore diameter values. The BET values calculated were 4.003 and 6.032 (m^2/g), whereas the pore volumes were 0.011 and 0.017 (cm^3/g) for the ZnO (without extract) and green ZnO NPs, respectively. Since the small porous samples had a large surface area, the behavior of the material as a whole may have begun to be dominated by its surface qualities; by comparison, the green ZnO was highly porous, and thus had a high surface area. Figure 9 show nitrogen adsorption–desorption isotherms of ZnO (without extract) and green ZnO NPs. where Figure 10 illustrates the common Barrett–Joyner–Halenda (BJH) desorption pore size distribution curves for the ZnO (without extract) and green ZnO NPs. The curves show that the majority of the mesoporous particles had a size of less than 40 nm.

Table 4. BET, pore volume, and pore distribution of ZnO (without extract) and green ZnO NPs.

Samples	BET (m^2/g)	Pore Volume (cm^3/g)	Average Pore Diameter (nm)
ZnO (without extract)	4.003	0.011	18.455
Green ZnO	6.032	0.017	15.876

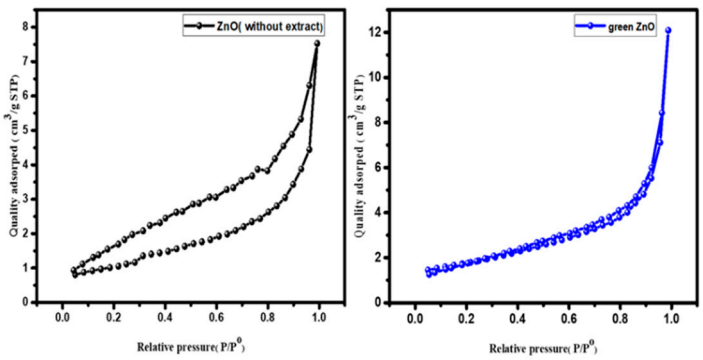

Figure 9. N_2 adsorption–desorption isotherms of ZnO (without extract) and green ZnO NPs.

Preprints (www.preprints.org) | NOT PEER-REVIEWED | Posted: 5 July 2023 doi:10.20944/preprints202307.0314.v1

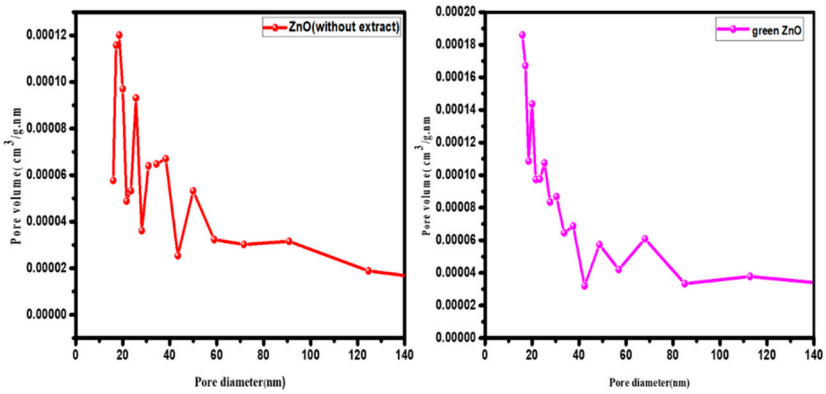

Figure 10. BJH pore size distribution curves for the ZnO (without extract) and green ZnO NPs

4. Conclusions

This study used a green technique to create ZnO NPs using *Artemisia absinthium* plant extract as a minimizing and stabilizing agent. The characteristics and quality of the green ZnO and ZnO (without extract) NPs were examined utilizing several analytical techniques. The study showed that the plant extract from *A. absinthium* efficiently performed a role in decreasing and stabilizing the NP samples that were prepared. The outcomes of this approach yielded spherical and hexagonal forms with average diameters of 18.77 and 24.39 nm for the green ZnO and ZnO (without extract) NPs, respectively. FTIR analysis confirmed the formation of NPs with the new broad absorption bands observed at 432.05 and 439.77 cm^{-1} for the green ZnO and ZnO (without extract) NPs, respectively. The band gap energy values narrowed from 2.79 to 2.65 between the ZnO (without extract) and green ZnO NPs, respectively.

The N_2 adsorption–desorption isotherms demonstrated that the pore volume on a given surface increased with an increasing surface area from 4.003 to 6.032 m^2/g. The pore volumes were from 0.011 to 0.017 cm^3/g, and the pore diameters were from 18.455 to 15.876 nm for the ZnO (without extract) and green ZnO NPs, respectively.

This research demonstrated that using a green approach can generate stable nano-sized ZnO particles while being cost-effective and yielding high-quality crystallization.

Author Contributions: Conceptualization F. A and Z. A; methodology, F. A; software, Z. A, formal analysis, F. A.; investigation, Z. A.; resources, F. A; data curation S. M.; writing—original draft preparation, F. A.; writing—review and editing, Z. A and S. M, supervision, Z.A. and S. M; project administration, Z. A.; funding acquisition, F. A. All authors have read and agreed to the published version of the manuscript.

Funding: This research received no external funding.

Institutional Review Board Statement: Not applicable

Informed Consent Statement: Not applicable

Data availability: All data are available on request.

Acknowledgments: The authors are grateful for the support of the Chemistry Department in the College of Science and Arts at Al-Rass, Qassim University.

Conflicts of Interest: All authors confirm that they do not have any conflicts of interest related to the research in this manuscript.

References

1. Rahman, F.; Majed Patwary, M.A.; Bakar Siddique, M.A.; Bashar, M.S.; Haque, M.A.; Akter, B.; Rashid, R.; Haque, M.A.; Royhan Uddin, A.K.M. Green synthesis of zinc oxide nanoparticles using Cocos nucifera leaf extract: Characterization, antimicrobial, antioxidant and photocatalytic activity. *R. Soc. Open Sci.* **2022**, *9*, 220858. https://doi.org/10.1098/rsos.220858.
2. Abdelbaky, A.S.; El-mageed, T.A.A.; Babalghith, A.O.; Selim, S.; Mohamed, A.M.H.A. Green Synthesis and Characterization of ZnO Nanoparticles Using *Pelargonium odoratissimum* (L.) Aqueous Leaf Extract and Their Antioxidant, Antibacterial and Anti-inflammatory Activities. *Antioxidants* **2022**, *11*, 1444.
3. Islam, F.; Shohag, S.; Uddin, J.; Islam, R.; Nafady, M.H. Exploring the Journey of Zinc Oxide Nanoparticles (ZnO-NPs) toward Biomedical Applications. *Materials* **2022**, *15*, 2160.
4. Faisal, S.; Jan, H.; Shah, S.A.; Shah, S.; Khan, A.; Akbar, M.T.; Rizwan, M.; Jan, F.; Wajidullah; Akhtar, N.; et al. Green Synthesis of Zinc Oxide (ZnO) Nanoparticles Using Aqueous Fruit Extracts of Myristica fragrans: Their Characterizations and Biological and Environmental Applications. *ACS Omega* **2021**, *6*, 9709–9722. https://doi.org/10.1021/acsomega.1c00310.
5. Karam, S.T.; Abdulrahman, A.F. Green Synthesis and Characterization of ZnO Nanoparticles by Using Thyme Plant Leaf Extract. *Photonics* **2022**, *9*, 594.
6. Sundrarajan, M.; Ambika, S.; Bharathi, K. Plant-extract mediated synthesis of ZnO nanoparticles using Pongamia pinnata and their activity against pathogenic bacteria. *Adv. Powder Technol.* **2015**, *26*, 1294–1299. https://doi.org/10.1016/j.apt.2015.07.001.
7. Wibowo, A.; Marsudi, M.A.; Amal, M.I.; Ananda, M.B.; Stephanie, R.; Ardy, H.; Diguna, L.J. ZnO nanostructured materials for emerging solar cell applications. *RSC Adv.* **2020**, *10*, 42838–42859. https://doi.org/10.1039/d0ra07689a.
8. Subhan, M.A.; Neogi, N.; Choudhury, K.P. Industrial Manufacturing Applications of Zinc Oxide Nanomaterials: A Comprehensive Study. *Nanomanufacturing* **2022**, *2*, 265–291. https://doi.org/10.3390/nanomanufacturing2040016.
9. Liewhiran, C.; Tamaekong, N.; Wisitsoraat, A.; Tuantranont, A.; Phanichphant, S. Sensors and Actuators B: Chemical Ultra-sensitive H 2 sensors based on flame-spray-made Pd-loaded SnO 2 sensing films. *Sens. Actuators B Chem.* **2013**, *176*, 893–905.
10. Lopez-Miranda, J.L.; Molina, G.A.; González-Reyna, M.A.; España-Sánchez, B.L.; Esparza, R.; Silva, R.; Estévez, M. Antibacterial and Anti-Inflammatory Properties of ZnO Nanoparticles Synthesized by a Green Method Using Sargassum Extracts. *Int. J. Mol. Sci.* **2023**, *24*, 1474. https://doi.org/10.3390/ijms24021474.
11. Djearamane, S.; Xiu, L.J.; Wong, L.S.; Rajamani, R.; Bharathi, D.; Kayarohanam, S.; De Cruz, A.E.; Tey, L.H.; Janakiraman, A.K.; Aminuzzaman, M.; et al. Antifungal Properties of Zinc Oxide Nanoparticles on Candida albicans. *Coatings* **2022**, *12*, 1864. https://doi.org/10.3390/coatings12121864.
12. Kumar Jangir, L.; Kumari, Y.; Kumar, A.; Kumar, M.; Awasthi, K. Investigation of luminescence and structural properties of ZnO nanoparticles, synthesized with different precursors. *Mater. Chem. Front.* **2017**, *1*, 1413–1421. https://doi.org/10.1039/c7qm00058h.
13. Pino, P.; Bosco, F.; Mollea, C.; Onida, B. Antimicrobial Nano-Zinc Oxide Biocomposites for Wound Healing Applications: A Review. *Pharmaceutics* **2023**, *15*, 970. https://doi.org/10.3390/pharmaceutics15030970.
14. Kumar, R. Polymer precursor method for the synthesis of zinc oxide nanoparticles: A Novel Approach. *Research Square*, **2023**, 1–12.
15. Fiedler, S.; Lee, L.O.; Lem, C.; Ton-that, C.; Schleuning, M.; Ho, A.; Phillips, M.R. Correlative Study of Enhanced Excitonic Emission in ZnO Coated with Al Nanoparticles using Electron and Laser Excitation. *Sci. Rep.* **2020**, *10*, 2553.
16. Bode, A.M.; Roh, E. Are FDA-approved sunscreen components effective in preventing solar UV-induced skin cancer? *Cells* **2020**, *9*, 1674.
17. Barcaui, C.B.; Gomes, E.E.; Lupi, O.; Marc, C.R. *Anais Brasileiros de Dermatologia*. **2022**, *97*, 204 -222.
18. Synthesis, N.; Harharah, H.N.; Elboughdiri, N.; Tahoon, M.A. Plant and Microbial Approaches as Green Methods for the Synthesis of Nanomaterials: Synthesis, Applications, and Future Perspectives. *Molecules* **2023**, *28*, 463.
19. Shah, M.; Fawcett, D.; Sharma, S.; Tripathy, S.K. Green Synthesis of Metallic Nanoparticles via Biological Entities. *Materials* **2015**, *8*, 7278–7308.

20. Meera, V.P.A.S.; Maria, C.G.A. Green synthesis of nanoparticles from biodegradable waste extracts and their applications : A critical review. *Nanotechnol. Environ. Eng.* **2022**, 8,377-397 https://doi.org/10.1007/s41204-022-00276-8.
21. Baig, N.; Kammakakam, I.; Falath, W. Nanomaterials: a review of synthesis methods, properties, recent progress, and challenges. *Mater. Adv.* **2021**, *2*, 1821–1871. https://doi.org/10.1039/d0ma00807a.
22. Rashid, I.M.; Salman, S.D.; Mohammed, A.K.; Mahdi, Y.S. Green Synthesis of Nickle Oxide Nanoparticles for Adsorption of Dyes. *Sains Malays.* **2022**, *51*, 533–546. https://doi.org/10.17576/jsm-2022-5102-17.
23. Bawazeer, S.; Rauf, A.; Uzair, S.; Shah, A.; Shawky, A.M.; Awthan, Y.S. Al Green synthesis of silver nanoparticles using Tropaeolum majus: Phytochemical screening and antibacterial studies. *Green Process. Synth.* **2021**, *10*, 85–94.
24. Kumar, R.; Fikadu, A.; Bachheti, A.; Husen, A. Saudi Journal of Biological Sciences Biogenic fabrication of nanomaterials from flower-based chemical compounds, characterization and their various applications: A review. *Saudi J. Biol. Sci.* **2020**, *27*, 2551–2562.
25. Adeyemi, J.O.; Oriola, A.O.; Onwudiwe, D.C. Plant Extracts Mediated Metal-Based Nanoparticles: Synthesis and Biological Applications. *Biomolecules* **2022**, *12*, 627.
26. Izwanie, N.; Basri, H.; Harun, Z. Heliyon Zinc oxide from aloe vera extract: Two-level factorial screening of biosynthesis parameters. *Heliyon* **2020**, *6*, e03156.
27. Ramzan, M.; Ayub, F.; Shah, A.A.; Naz, G.; Shah, A.N.; Malik, A.; Sardar, R.; Telesiński, A.; Kalaji, H.M.; Dessoky, E.S.; et al. Synergistic Effect of Zinc Oxide Nanoparticles and Moringa oleifera Leaf Extract Alleviates Cadmium Toxicity in Linum usitatissimum: Antioxidants and Physiochemical Studies. *Front. Plant Sci.* **2022**, *13*, 900347. https://doi.org/10.3389/fpls.2022.900347.
28. Stan, M.; Popa, A.; Toloman, D.; Silipas, T.D.; Vodnar, D.C. Antibacterial and antioxidant activities of ZnO nanoparticles synthesized using extracts of Allium sativum, Rosmarinus officinalis and Ocimum basilicum. *Acta Metall. Sin. Engl. Lett.* **2016**, *29*, 228–236. https://doi.org/10.1007/s40195-016-0380-7.
29. Noukelag, S.K.; Mohamed, H.E.A.; Moussaa, B.; Razanamahandry, L.C.; Ntwampe, S.K.O.; Arendse, C.J.; Maaza, M. Investigation of structural and optical properties of biosynthesized Zincite (ZnO) nanoparticles (NPs) via an aqueous extract of Rosmarinus officinalis (rosemary) leaves. *MRS Adv.* **2020**, *5*, 2349–2358. https://doi.org/10.1557/adv.2020.220.
30. Iqbal, Y.; Raouf Malik, A.; Iqbal, T.; Hammad Aziz, M.; Ahmed, F.; Abolaban, F.A.; Mansoor Ali, S.; Ullah, H. Green synthesis of ZnO and Ag-doped ZnO nanoparticles using Azadirachta indica leaves: Characterization and their potential antibacterial, antidiabetic, and wound-healing activities. *Mater. Lett.* **2021**, *305*, 130671. https://doi.org/10.1016/j.matlet.2021.130671.
31. US, P.; Pujar, A.; Yadawe, M. Study on Green Synthesis, Characterization and Anticancer Activity of Thorium Nanoparticles Using Tomato (Lycopersicon Esculentum) Extract. *IOSR J. Appl. Chem.* **2018**, *11*, 25–29. https://doi.org/10.9790/5736-1107032529.
32. Gutiérrez-Miceli, F.A.; Oliva-Llaven, M.Á.; Luján-Hidalgo, M.C.; Velázquez-Gamboa, M.C.; González-Mendoza, D.; Sánchez-Roque, Y. Zinc Oxide Phytonanoparticles' Effects on Yield and Mineral Contents in Fruits of Tomato (Solanum lycopersicum L. cv. Cherry) under Field Conditions. *Sci. World J.* **2021**, *2021*, 5561930. https://doi.org/10.1155/2021/5561930.
33. Bhat, R.R.; Rehman, M.U.; Shabir, A.; Mir, M.; Ahmad, A.; Khan, R.; Masoodi, M.H.; Madkhali, H.; Ganaie, M.A. Chemical Composition and Biological Uses of *Artemisia absinthium* (Wormwood). In *Plant and Human Health*; Springer: Berlin/Heidelberg, Germany, 2019; Volume 3. https://doi.org/10.1007/978-3-030-04408-4_3.
34. Allemailem, K.S. Aqueous Extract of Artemisia annua Shows In Vitro Antimicrobial Activity and an In Vivo Chemopreventive Effect in a Small-Cell Lung Cancer Model. *Plants* **2022**, *11*, 3341.
35. Monirian, F.; Abedi, R.; Balmeh, N.; Mahmoudi, S.; Mirzaei, F. In-vitro antibacterial effects of Artemisia extracts on clinical strains of *P. aeruginosa*, *S. pyogenes*, and oral bacteria. *Jorjani Biomed. J.* **2020**, *8*, 35–43. https://doi.org/10.29252/jorjanibiomedj.8.3.35.
36. Ikram, M.A.M.; Ul, M.I.A.; Avais, H.M. Green synthesis and evaluation of n-Type ZnO nanoparticles doped with plant extract for use as alternative antibacterials. *Appl. Nanosci.* **2020**, *10*, 3787–3803.
37. Vera, J.; Herrera, W.; Hermosilla, E.; Díaz, M.; Parada, J.; Seabra, A.B.; Tortella, G.; Pesenti, H.; Ciudad, G.; Rubilar, O. Antioxidant Activity as an Indicator of the Efficiency of Plant Extract-Mediated Synthesis of Zinc Oxide Nanoparticles. *Antioxidants* **2023**, *12*, 784. https://doi.org/10.3390/antiox12040784.

38. Jayachandran, A.; Aswathy, T.R.; Nair, A.S. Green synthesis and characterization of zinc oxide nanoparticles using Cayratia pedata leaf extract. *Biochem. Biophys. Rep.* **2021**, *26*, 100995.
39. Srivastava, V.; Gusain, D.; Sharma, Y.C. Synthesis, characterization and application of zinc oxide nanoparticles (n-ZnO). *Ceram. Int.* **2013**, *39*, 9803–9808. https://doi.org/10.1016/j.ceramint.2013.04.110.
40. Hajiashra, S.; Motakef, N. Heliyon Preparation and evaluation of ZnO nanoparticles by thermal decomposition of MOF-5. *Heliyon* **2019**, *5*, e02152.
41. Demissie, M.G.; Sabir, F.K.; Edossa, G.D.; Gonfa, B.A. Synthesis of Zinc Oxide Nanoparticles Using Leaf Extract of *Lippia adoensis* (Koseret) and Evaluation of Its Antibacterial Activity. *J. Chem.* **2020**, *2020*, 7459042.
42. Faisal, M.; Bahadar, S.; Rahman, M.M.; Jamal, A.; Abdullah, M.M. Applied Surface Science Fabrication of ZnO nanoparticles based sensitive methanol sensor and efficient photocatalyst. *Appl. Nanosci.* **2012**, *258*, 7515–7522.
43. Kumar, S.S.; Venkateswarlu, P.; Rao, V.R.; Rao, G.N. Synthesis, characterization and optical properties of zinc oxide nanoparticles. *Int. Nano Lett.* **2013**, *3*, 30.
44. Suresh, D.; Nethravathi, P.C.; Rajanaika, H. Materials Science in Semiconductor Processing Green synthesis of multifunctional zinc oxide (ZnO) nanoparticles using Cassia fistula plant extract and their photodegradative , antioxidant and antibacterial activities. *Mater. Sci. Semicond. Process.* **2015**, *31*, 446–454.
45. Taha, K.K.; Zoman, M.; Al Outeibi, M.; Al Modwi, S.A.A.; Bagabas, A.A. Green and sonogreen synthesis of zinc oxide nanoparticles for the photocatalytic degradation of methylene blue in water. *Nanotechnol. Environ. Eng.* **2019**, *4*, 10.